THE JOURNAL OF PHYSICAL CHEMISTRY B

ARTICLE

pubs.acs.org/JPCB

Thermodynamics of Hyperbranched Poly(ethylenimine) with Isobutyramide Residues during Phase Transition: An Insight into the Molecular Mechanism

Hongna Wang, Shengtong Sun, and Peiyi Wu*

The Key Laboratory of Molecular Engineering of Polymers, Ministry of Education, Department of Macromolecular Science, and Laboratory of Advanced Materials, Fudan University, Shanghai 200433, People's Republic of China

ABSTRACT: The thermodynamic behavior of hyperbranched poly(ethylenimine) with isobutyramide groups (HPEI-IBAm) during thermal-induced phase transition in water was investigated by turbidity measurement, calorimetric measurements (DSC), FT-IR, and dynamic light scattering (DLS). Both turbidity and calorimetric measurements indicated a recoverable phase transition with a small hysteresis. Detailed FT-IR investigation gave an insight into its molecular mechanism about detailed group interaction during the heating−cooling process. The second derivative and Gaussian fit were carried out to separate three components of ν(C═O): 1648, 1625, and 1600 cm^{-1}, which are assigned to C═O···D—N H-bonds, single and double H-bonded carbonyl groups with water molecules, respectively. Quantitative analysis of amide I groups indicates a better revival compared to PNIPAM. The isosbestic point determination and 2D correlation analysis together with dynamic light scattering were applied to draw out the mechanism. Thermosensitive HPEI-IBAm dissolves in water exhibits small particles of ca. 3 nm at room temperature at first. As temperature increases, the polymer begins to shrink and water is driven out from the polymer. Finally, the polymer results in a hydrophobic sphere, which aggregates further for a relative stable state upon heating. Above LCST, C═O···D—N hydrogen bonds form with the disassociation of C═O···D_2O, which helps in the dehydration of CH groups. Upon cooling, the driven force of the transition is the hydration of CH groups. Compared with linear-PNIPAM, the globule-like hyperbranched polymer has a high specific area which endows the groups with a high degree of freedom and more sufficient interaction with water.

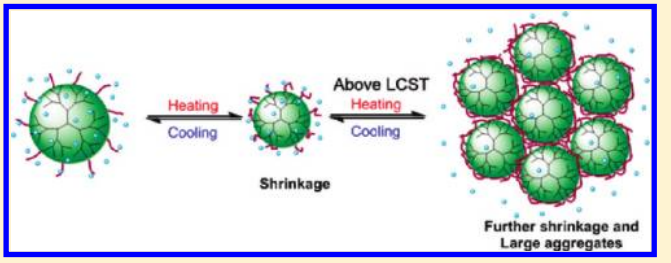

1. INTRODUCTION

Hyperbranched polymer is a type of dendritic polymer which holds similar properties as dendrimer: large numbers of terminal functional groups for design, low solution viscosity, and excellent solubility compared to linear polymers.[1−5] Due to their unique chemical and physical properties, hyperbranched polymers are of great potential applications in coatings,[6] additives,[2] drug and gene delivery,[7−9] macromolecular building blocks,[10,11] nanotechnology,[12,13] supramolecular science, etc.[3]

Polymers that exhibit environmentally responsive behavior such as temperature,[14] pH,[15] and light[16] have attracted great interest, especially thermosensitive polymers having the lower critical solution temperature (LCST) in aqueous solution. Below the LCST, the polymers are well soluble in water and adopt an extended chain conformation. As temperature increases, the polymers tend to collapse and become insoluble above LCST.[17] One of the most extensively investigated thermosensitive polymers in water is poly(*N*-isopropylacrylamide) (PNIPAM). The repeating units of PNIPAM are composed of hydrophilic (amide) and hydrophobic (isopropyl) groups with an LCST of approximately 32 °C.[18] Besides PNIPAM, other *N*-alkyl-substituted polymers such as poly(*N*,*N*-dialkylacrylamide)s,[19] and poly(*N*-vinylisobutylamide)s[20] are also well studied. Modified polymers such as block,[21] star,[22] and graft[23] polymers based on linear thermosensitive unit are widely studied as well. Nevertheless, the LCST property of these modified polymers is independent of their specific topology but just contributed by their thermosensitive unit.

Recently, researches of dendrimer and hyperbranched polymers with an LCST that are dependent on their globule-like shapes are reported. Poly(amidoamine) (PAMAM) dendrimers were modified with various alkylamide groups,[24] such as isobutyramide (IBAm) groups,[25] to be thermoresponsive by the Kono group. The IBAm terminated dendrimer exhibits more remarkable molecular weight dependence compared with linear polymer; an increase in the molecular weight of ca. 9150 to ca. 37 800 causes about 30 °C decrease in the LCST. By comparison of *N*-isopropylamide-bearing dendrimers with linear polymers, marked differences in transition enthalpy, hydrophobicity, and sensitivity were found due to their structural features.[26] They also introduce succinic anhydride and isopropylamine,[27] oligo(ethylene glycol) monoethers[28] to make poly(glycidol)s pH or thermal sensitive. Moreover, the Yan group introduced 1-adamantylamine,[29] adamantyl,[30] etc. to hyperbranched polymer to endow it with thermo- and pH-responsive properties and host/guest interaction. Together with what is mentioned above, the Chen group has also done researches on thermo- and

Received: January 27, 2011
Revised: June 8, 2011
Published: June 09, 2011

pH-sensitive hyperbranched poly(ethylenimine)s with isobutyramide groups (HPEI-IBAm).[31−34] They modified terminal amine groups with isobutyramide groups to introduce a hydrophilic−hydrophobic balance. The balance will be broken with the variation of temperature or pH, which in turn results in phase transition. The LCST of HPEI-IBAm is much more sensitive to molecular weight alteration than dendrimer analogues and can be adjusted conveniently by varying the molecular weight of the HPEI precursor, the acidity of the aqueous media, or the degree of amidation. Combining HPEI-IBAm with gold nanoparticles will endow the nanoparticles with thermosensitivity so that the nanoparticles can be used as a color sensor and catalyst. Chen et al. have compared the differences of factors' influence on LCST among hyperbranched polymer, dendrimer, and linear polymers. However, detailed information on the molecular mechanism of the phase transition process has not been discussed. Furthermore, HPEI is one of the most efficient nonviral gene-transfection agents, especially the commercially available branched PEI (M_n = 25 000 g/mol). It has been widely used as "gold standard" for evaluation of transfection efficiency of other newly developed polymer- or surfactant-based gene carriers.[35−37] For its extensively applications in gene therapy, we think it of great importance to make a detailed study on the thermal behavior of HPEI-IBAm in water. To date, there have been many researches focusing on the phase transition mechanism of polymer holding an LCST. However, to the best of our knowledge, most of these researches are about the linear polymeric system,[14,19,38−45] especially PNIPAM.[43−46] There is almost no detailed study on LCST behavior of hyperbranched polymer. Very recently, the Yan group[13] reported a study on molecular mechanism of temperature-responsive phase transition of polymer vesicles with hyperbranched polymer as the core. However, their researches[47,48] are mainly concerned with assembly mechanism on a relative large scale rather than detailed groups' interaction mechanism during environmental changes. In addition, temperature-dependent phase transition molecular mechanism of HPEI-IBAm, a hyperbranched polymer, has not been proposed yet.

In this paper, we aim to figure out the microdynamic phase transition mechanism of HPEI-IBAm aqueous solution mainly using FT-IR spectroscopy, in combination with DSC, turbidity, and DLS measurements. Results from DSC and turbidity measurements will provide an appropriate temperature range to perform FT-IR experiment and give information about the phase transition such as LCST, the extent of the phase transition revival, etc. Then a detailed FT-IR analysis can help us to get an insight into the molecular motion and interactions between groups with perturbation correlation moving window (PCMW) and 2D correlation spectroscopy (2Dcos). PCMW is a technique that will not only determine the transition point but also monitor the complicated spectral variations along the perturbation direction. 2Dcos is a mathematical method which can improve the resolution of 1D spectrum and provide information about molecular motions. Then, in order to derive a mechanism reasonably, dynamic light scattering has been applied to draw the macroscopic profiles about how the molecules exist in aqueous solution.

2. EXPERIMENTAL SECTION

2.1. Materials. Hyperbranched pol(ethylenimine), HPEI-1.8K (Alfa Aesar) was dried under vacuum before use. Isobutyric anhydride, dichloromethane, triethylamine (TEA), sodium chloride, sodium carbonate, and anhydrous sodium sulfate were purchased from Shanghai Jingchun Chemical Reagent Co. Ltd. and used without further purification unless stated otherwise. Benzoylated cellulose membrane (MWCO 1000 g/mol) was purchased from Shanghai Greenbird Co. Ltd. and used after washing with deionized water.

Scheme 1. Synthesis of Hyperbranched Polymers with Isobutyric Amide (IBAm) Functional Groups (HPEI-IBAm) from Hyperbranched Polyethylenimine

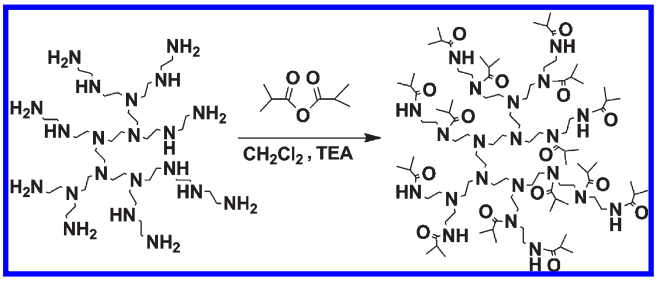

The preparation of HPEI-IBAm is similar to that reported,[34] but with a little modification. Under nitrogen atmosphere, isobutyric anhydride (10.175 g) was added dropwise to the mixture of HPEI (3.875 g) and TEA (6.95 g) in 50 mL of dichloromethane at 0 °C. The solvent here is replaced by dichloromethane for higher yield with lower viscosity during washing. The reaction mixture was then kept at room temperature. Finally, the reaction temperature was raised to 42 °C to complete the reaction. After washing with 10% $NaHCO_3$ and saturated NaCl solution, the mixture was dried by adding anhydrous Na_2SO_4 for 24 h. Volatiles were removed under vacuum and the residue was dissolved in methanol. Dialysis against methanol was performed. Finally, the solvent was removed under vacuum and dried in vacuum at 35 °C for 24 h. The degree of amidation is 94.2% calculated from ^{1}HNMR spectra (Scheme 1).

D_2O was purchased from Cambridge Isotope Laboratories Inc. (D-99.9%). The concentration of HPEI-IBAm aqueous solution was fixed at different concentrations for comparison in turbidity and dynamic laser scattering measurement. For FT-IR and DSC experiments, the concentration was fixed at 10 wt %. HPEI-IBAm was dissolved in D_2O and the solution was kept at 4 °C for a week before FT-IR experiments to ensure completely deuteration of all the NH protons.

2.2. Measurements. Turbidity measurements were carried out at 500 nm on a Lamda 35 UV−vis spectrometer with deionized water as reference (100% transmittance). Temperatures were regulated manually with a water-jacketed cell holder at the rate of ca. 0.5 °C/min with an increment of 0.5 °C. To ensure thermal equilibrium of the sample cell, each temperature point was held for 2 min before measurements. Calorimetric measurements were performed on a Mettler-Toledo differential scanning calorimeter thermal analyzer with a rate of 10, 5, and 1 °C/min during both heating and cooling process. The sample was prepared by sealing HPEI-IBAm solution between two CaF_2 tablets for FT-IR measurements. All time-resolved FT-IR spectra were recorded with a resolution of 4 cm^{-1} on a Nicolet Nexus 470 spectrometer equipped with a DTGS detector by signal-averaging 32 scans. Manual method was used to control the temperature at rates of ca. 0.3 °C/min with an increment of 0.5 °C. The baseline correction process was made by the software Omnic, ver. 6.1a. Dynamic light scattering was conducted on

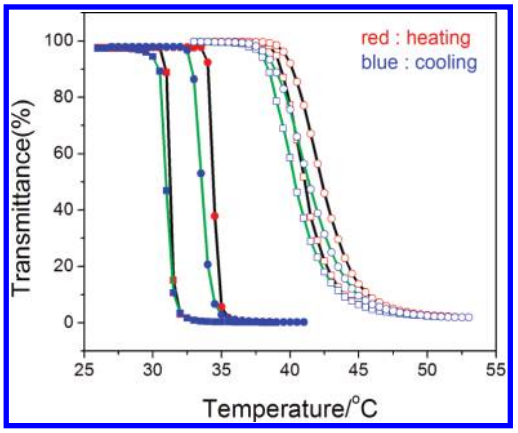

Figure 1. Plots of transmittance vs temperature for 1 wt % (solid squares), 0.5 wt % (solide circles), 0.1 wt % (hollow squares), and 0.05 wt % (hollow circles) of HPEI-IBAm in H_2O during the heating−cooling cycle.

a Malvern Zetasizer Nano ZS instrument between 25 and 40 °C with an interval of 1 °C and maintained for 2 min at each temperature point before measurements.

2.3. Investigation Methods. *2.3.1. Perturbation Correlation Moving Window (PCMW).* FT-IR spectra collected with an interval of 0.5 °C during the heating and cooling (27−39 °C) process were used to perform 2D correlation analysis, respectively. Primary data processing was carried out with the method Morita provided, and further correlation calculation was performed using the software 2D Shige, ver. 1.3 (Shigeaki Morita, Kwansei-Gakuin University, Japan, 2004−2005). The final contour maps were plotted by Origin program, ver. 8.0, with warm colors (red and yellow) defined as positive intensities and cool colors (blue) as negative ones. An appropriate window size ($2m$ + 1 = 11) was chosen to generate PCMW spectra with good quality.

2.3.2. 2D Correlation Spectroscopy (2Dcos). FT-IR spectra used for PCMW analysis were also used to perform 2D correlation analysis. 2D correlation analysis was carried out using the same software 2D Shige ver. 1.3 (Shigeaki Morita, Kwansei-Gakuin University, Japan, 2004−2005), and was further plotted into the contour maps by Origin program ver. 8.0. In the contour maps, warm colors (red and yellow) are defined as positive intensities, while cool colors (blue) are defined as negative ones.

3. RESULTS AND DISCUSSION

3.1. Turbidity and Calorimetric measurements. The phase transition behavior of HPEI-IBAm aqueous solution is first investigated by turbidity measurements. For comparison and determination of cloud points at different concentrations, HPEI-IBAm solutions of 1, 0.5, 0.1, and 0.05 wt % in H_2O were chosen. The solutions were measured during the heating−cooling cycle with an interval of 0.5 °C, as shown in Figure 1.

The cloud point is taken as the initial turn point in the transmittance versus temperature curves. It is clear that the phase transition is sharp with a small hysteresis. For 1 wt % aqueous solution, the cloud point during the cooling process is 29.5 °C which is ca. 1 °C lower than that during the heating process, 30.5 °C. However, as the polymer solutions are diluted to lower concentrations, the cloud point of both heating and cooling process increases and with a relatively broader transition range. This phenomenon is consistent with what was reported

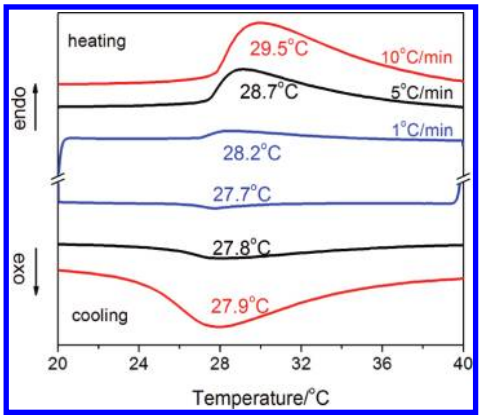

Figure 2. DSC thermograms of HPEI-IBAm aqueous solution at temperature variation rates of 10, 5, and 1 °C/min.

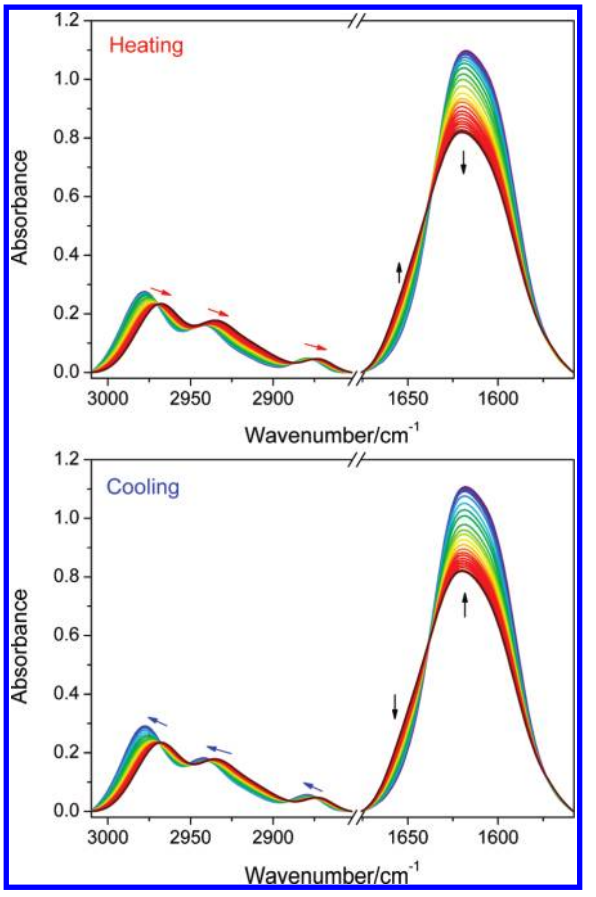

Figure 3. Temperature-dependent FT-IR spectra of 10 wt % HPEI-IBAm in D_2O (27−39 °C) during heating and cooling with an interval of 0.5 °C.

previously,[32] where the cloud point of HPEI-IBAm also increases with the decrease of polymer concentration.

Subsequently, DSC was performed to determine the phase transition process, shown in Figure 2. Rates of temperature variations at 10, 5, and 1 °C/min were chosen. The hyperbranched polymer represents the phase transition temperature (T_p) at 29.5 and 27.9 °C during the heating and the cooling process with rates of 10 °C/min, respectively. A similar small hysteresis is observed at all rates, which is consistent with turbidity measurements. But changing temperatures at lower

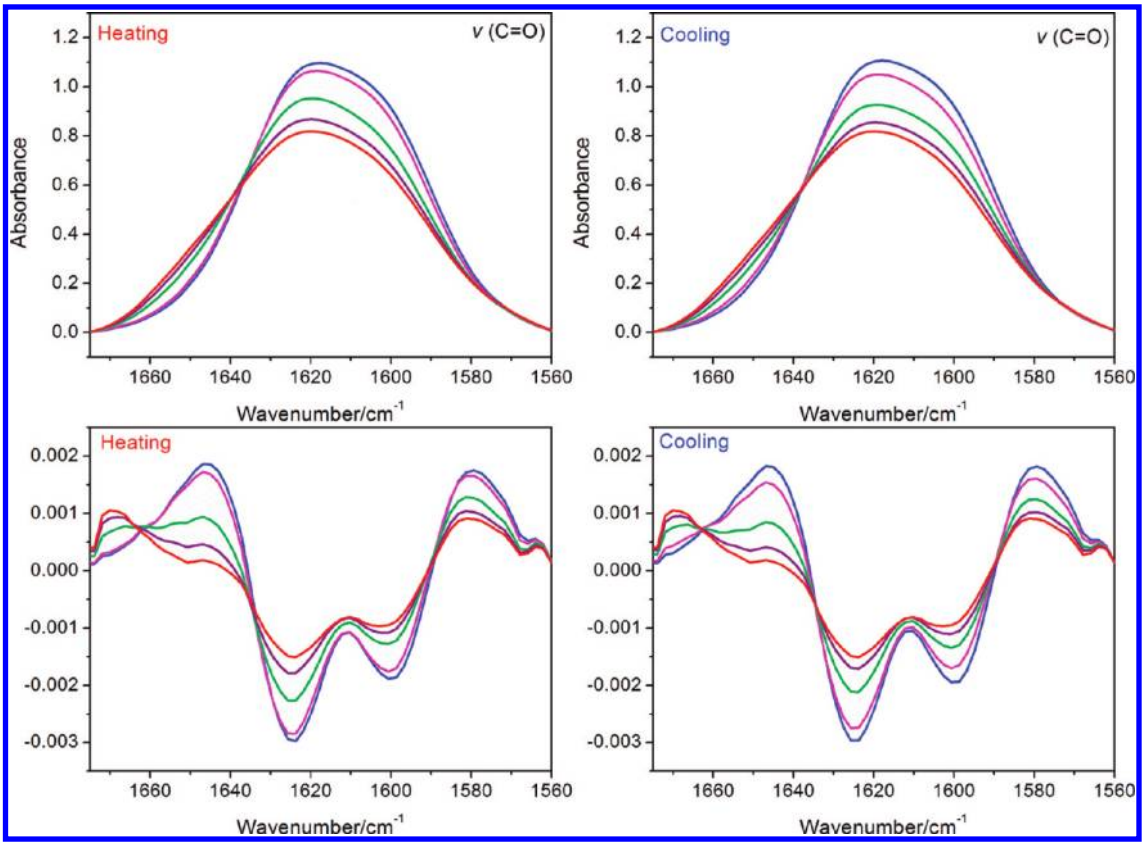

Figure 4. IR and second-derivative spectra of 10 wt % HPEI-IBAm measured in D_2O during the heating−cooling cycle.

rate narrows the gap between T_p of heating and cooling. If we perform the heating−cooling cycle at a rate low enough to achieve the complete thermodynamic equilibrium of HPEI-IBAm in water, the T_p we get from heating and cooling seem to be the same. However, it takes time to reach a system's thermodynamic equilibrium and without enough necessity. By the way, a lower rate leads to a relative lower T_p in both heating and cooling process is logically understood.

3.2. Conventional IR Analysis. D_2O, rather than H_2O, was selected as the solvent to eliminate the overlap of the δ(OH) band of water at about 1640 cm^{-1} with the amide I band, as well as the wavenumber interference of ν(OH) of H_2O in ν(CH) of HPEI-IBAm. Sample concentration was fixed at 10 wt % for reasonable signal-to-noise ratio of the FT-IR spectra. All spectra were collected between 27 and 39 °C to observe the entire phase transition process with an increment of 0.5 °C, as presented in Figure 3, wherein only two regions(C−H stretching bands in 3010−2854 cm^{-1}, and C═O stretching band or amide I in 1675−1560 cm^{-1}) are shown for detailed study.

As shown in Figure 3, upon heating, all the C−H groups shift to lower frequency and the C═O region exhibits a bidirectional spectral intensity changes. The spectra of the cooling process seem to show an opposite trend of changes to that in the heating process at the first glance. The changes of ν(CH) can be explained by the interactions between the hydrophobic moiety of the polymer and water molecules in solution. The more water molecules around it, the higher the frequency is.[14,49] From this point, it can be deduced that, as the hydrophobic parts, the CH groups dehydrate with the increase of temperature and hydrate again while cooling down, which is a common phenomenon in phase transition system of water-soluble polymers. Referring to the ν(C═O) band, it can be separated into two parts: the lower frequency moiety and the higher one. The intensity of the lower frequency moiety decreases with the higher one increasing upon heating, and changes during the cooling process seem contrary. In a similar system of PNIPAM, which also holds amide groups, the ν(C═O) was combined by two bands at 1650 and 1625 cm^{-1}, which can be attributed to C═O···D—N and C═O···D_2O hydrogen bonds, respectively.[14,49] However, there seems to be a "shoulder" band around 1600 cm^{-1} besides the two bands mentioned above.

To find out whether the ν(C═O) here is the same as that of PNIPAM, enlarged spectra of ν(C═O) band region are presented in Figure 4. The second-derivative analysis is applied in order to separate the overlapped bands. The sharpened minima in the second derivative correspond to the maxima in the original absorption spectra. The peak positions of three bands at 1648, 1625, and 1600 cm^{-1} are determined by second-derivative spectra. Here, a band at 1600 cm^{-1} was newly observed besides the other two bands discussed previously. It is well-known that ν(C═O) shifts toward lower wavenumbers when the carbonyl group is hydrogen bonded.[50,51] The 1600 cm^{-1} band can be assigned to doubly H-bonded carbonyl groups with water molecules.[46] Then, the responses of carbonyl groups during phase transition can be described as follows. Upon heating, singly and doubly bonded hydrogens of C═O···D_2O break with the formation of C═O···D—N hydrogen bonds. Inverse changes appear during cooling process. Based on all the discussions about the conventional IR spectra, it may be concluded that the transition here is reversible.

dx.doi.org/10.1021/jp2008682 |J. Phys. Chem. B 2011, 115, 8832–8844

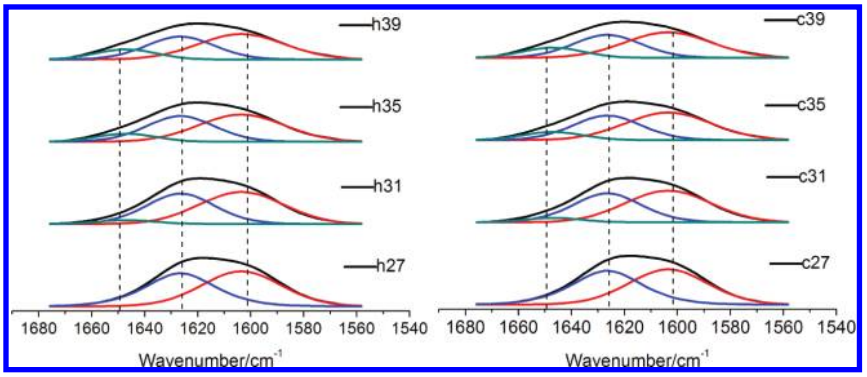

Figure 5. Baseline-corrected ν(C═O) bands measured during the heating and cooling process. The color lines indicate the Gaussian fit to separate different components.

For further study, the ν(C═O) band is fitted with Gaussian curves according to the results of the second derivative, as presented in Figure 5. Here, spectra at four different temperatures during the heating and cooling process are chosen as examples, respectively. Curve fitting reveals that two or three bands are necessary to match the spectra at different temperatures satisfactorily. Due to second-derivative analysis, two bands at 1600 and 1625 cm^{-1} exist at lower frequency contributed from singly and doubly H-bonded carbonyl groups with water molecules below LCST. As temperature increases, a third band at 1648 cm^{-1} appears and increases gradually, which is the evidence of another form of C═O groups. As is known, the band at 1648 cm^{-1} can usually be assigned to the C═O···D—N hydrogen bonds in a similar system such as PNIPAM aqueous solution containing amide groups and water molecules.[14,52] So the results can be described as that the hydrogen bonds from inner/inter-amide groups begin to form above the LCST upon temperature increases.

It should be pointed out that the area experiences an obvious variation upon cycling up and down in temperature. In conjunction with Figures 4 and 5, one can discern by eye that the total area of the bands region of amide I groups decreases with the bidirectional change mentioned above during the heating process. The bidirectional change contains an apparent decrease in the absorbance of the lower frequency components and a relative small increase of the higher frequency. As is known to all, the area reflects the relative content of the groups. Then, one may wonder why there is a decrease in total area without "missing any carbonyl groups". In fact, the integration area is equal to absorbance in a sense, and the absorbance can be described according to the Beer−Lambert law:

$$I_i = a_i bc$$

where a_i is the absorption coefficient, b is the path length, and c represents the concentration of the species. In our studies, we do not know the absolute value of b, but it is constant throughout the investigations. Absorbance changes of three components belong to the ν(C═O) band during the heating and cooling process are shown in Figure 6. The areas of both 1600 and 1625 cm^{-1} bands decrease during heating while the area of the 1648 cm^{-1} band increases. As the total area decreases finally, one can deduce that the area increment of 1648 cm^{-1} cannot make up all the decrement which corresponds to 1600 and 1625 cm^{-1}. The absorption coefficient a_i should be a strong function of frequency according to previous study.[53] The three components here at

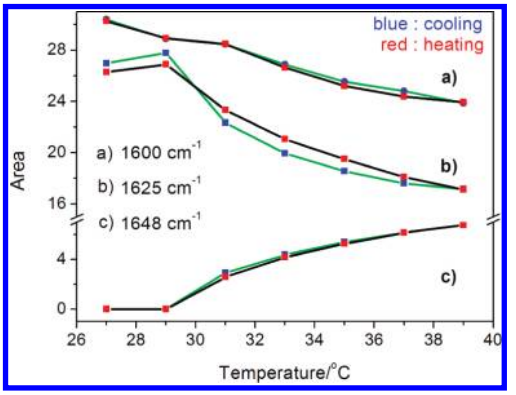

Figure 6. Integration area of bands at 1600, 1625, and 1648 cm^{-1} vs temperature during the heating and cooling process.

different frequency will have different a_i. So the total area decrement is owing to a smaller a_i of 1648 cm^{-1} than 1600 and 1625 cm^{-1} attributed to C═O···D—N hydrogen bonds and H-bonds between C═O and D_2O, respectively.

Attempts on quantitative analysis of relative content or fraction of each component seem to be difficult because of the complicated changes during temperature variations. However, Figure 6 presents a quantitative analysis of each component's area variation versus temperature. Hydrogen bonds between C═O and D_2O dissociate upon heating with the formation of C═O···D—N hydrogen bonds. A good revival can be obtained with a small, if any, hysteresis during the cooling process. Hydrogen bonds of C═O···D—N break with the decrease of temperature and finally return to zero. It provides a significant difference with the linear PNIPAM system,[14] where the value of f(C═O···D—N) does not return to zero even when the temperature is far below the LCST. The phenomenon can be interpreted that there are entangled chains and strong C═O···D—N hydrogen-bond interactions in the concentrated solution which prevent the system from reversing to its original state, considering that HPEI-IBAm is a hyperbranched polymer and holds a globule-like topology which gives it a high specific surface area. Groups of hyperbranched polymer can interact with the environment with much more freedom than linear polymer in entangled coils. In addition, there are two kinds of amide, secondary and tertiary amide, with a ratio of 37:35 referring to the structure of HPEI-IBAm. Only secondary amide groups can afford proton to form hydrogen bonds with carbonyl groups. So

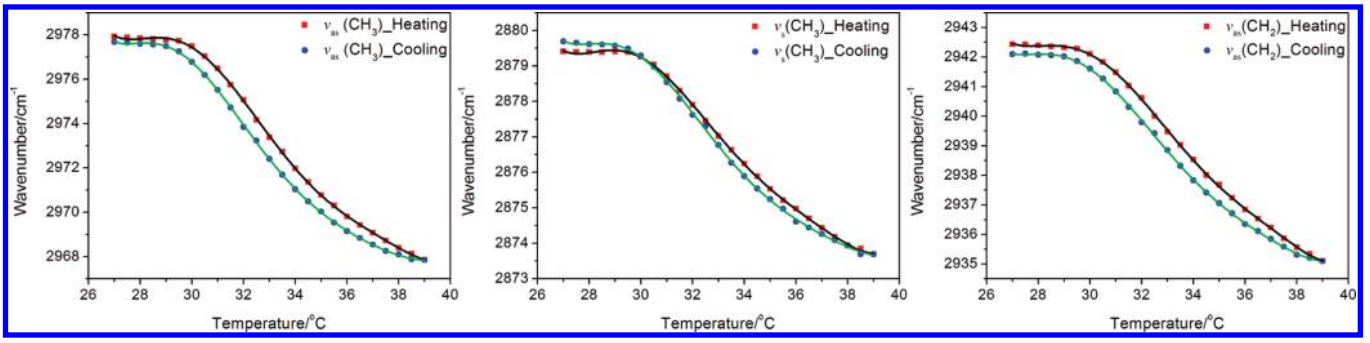

Figure 7. Temperature-dependent frequency shift of $\nu_{as}(CH_3)$, $\nu_{as}(CH_2)$, and $\nu_s(CH_3)$ in D_2O during heating and cooling.

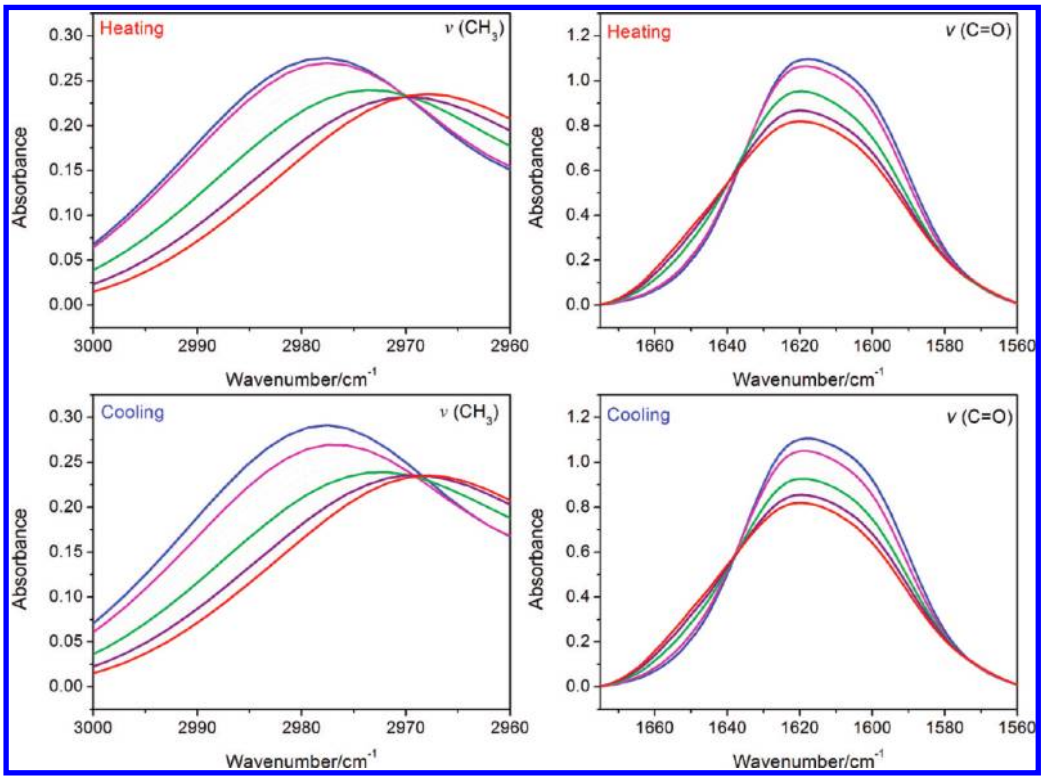

Figure 8. Determination of isosbestic points of $\nu(CH_3)$ and $\nu(C{=}O)$ overlaid spectra during heating and cooling. Three curves at 27, 30, 33, 36, and 39 °C are highlighted for better observation.

hydrogen bond of C═O···D—N intra/interhyperbranched polymer should be less and in a relative low density than polymer with all amide groups of the secondary one. In other words, spaces without C═O···D—N hydrogen bonds may seem as "defect" and promote water's diffusion into polymer during the cooling process. Consequently, hydrogen bond of C═O···D—N will disassociate more easily than that in PNIPAM and return to zero finally after cooling.

To determine the variations of C—H groups during heating—cooling circle, the temperature-dependent frequency shift of $\nu(CH)$ is shown in Figure 7. For clarity, nonlinear curve fitting is performed. An inconspicuous hysteresis is noticed. According to the globule-like structure, the CH groups are of relative high freedom and can dehydrate or hydrate freely with water during the heating—cooling process. CH_3 groups lie in the outer position of the globule-like polymer than CH_2 and have higher degree of freedom. So it shows a better revival during heating—cooling cycle from Figure 7.

Generally speaking, an isosbestic point occurs in overlaid spectra only when one component is quantitatively converted to another component.[54] To find whether the isosbestic point exists in the region of $\nu_{as}(CH)$ and $\nu(C{=}O)$, enlarged spectra of these regions with five highlighted curves with equal interval of temperatures, 27, 30, 33, 36, and 39 °C, are shown in Figure 8.

Interestingly, isosbestic points only existed in the $\nu_{as}(CH_3)$ region at 2970 cm^{-1} during heating and $\nu(C{=}O)$ region at 1638 cm^{-1} during cooling. It is very different from the PNIPAM aqueous solution (20 wt %) which shows isosbestic points in both heating and cooling processes.[14] Upon heating, CH_3 groups convert from hydrated state to dehydrated state without any intermediates, but the hydrogen bonds of C═O···D—N form with gradual disassociation of C═O···D_2O hydrogen bonds.

dx.doi.org/10.1021/jp2008682 |J. Phys. Chem. B 2011, 115, 8832–8844

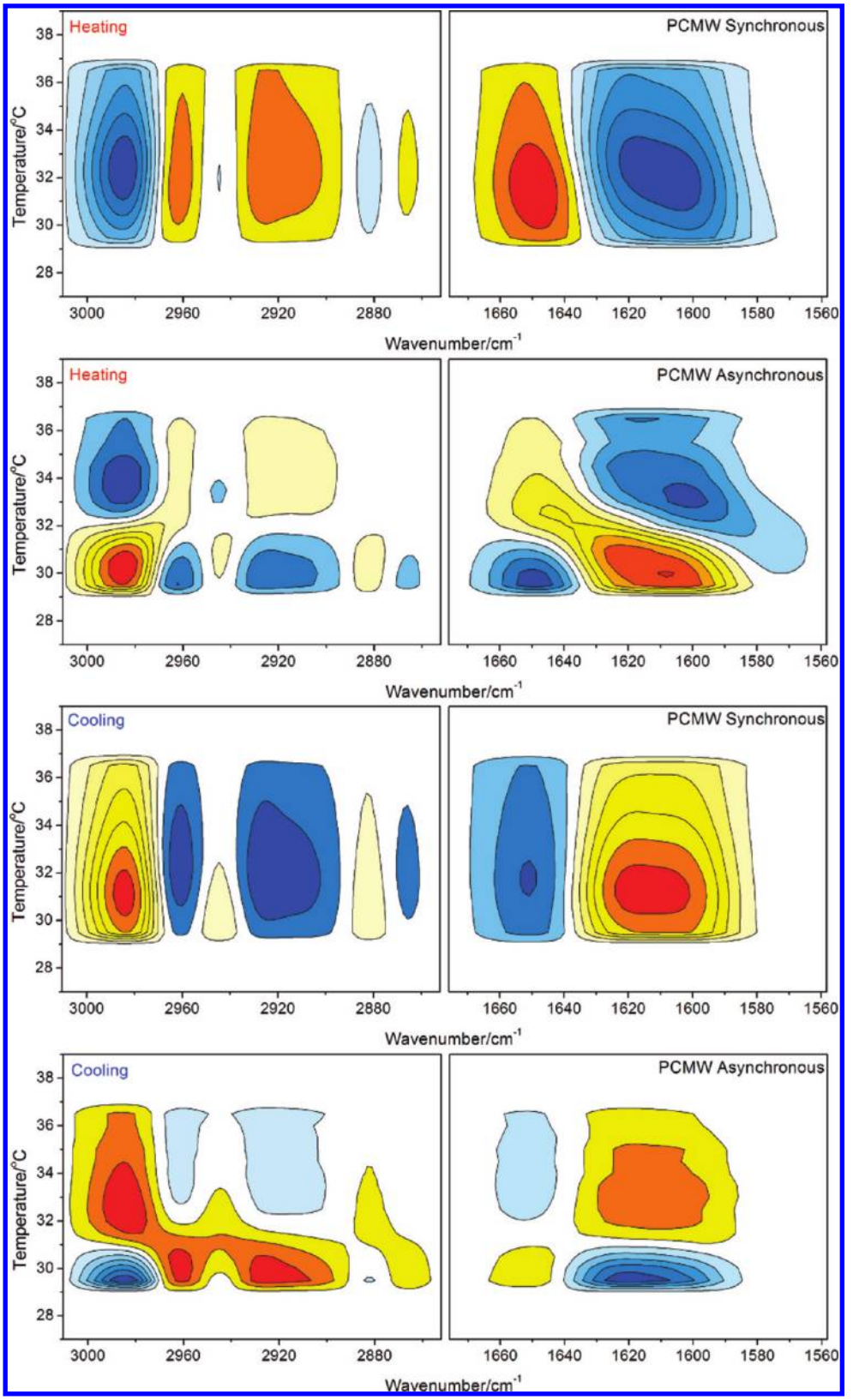

Figure 9. PCMW synchronous and asynchronous spectra of 10 wt % HPEI-IBAm in D_2O from all spectra between 27 and 39 °C during heating (top) and cooling (bottom). Warm colors (red and yellow) are defined as positive intensities, while cool colors (blue) as negative ones.

However, in the cooling process, the situation is the opposite. The C═O···D—N hydrogen bonds disassociate with the formation of C═O···D_2O hydrogen bonds without any intermediates, while hydration of CH_3 undergoes gradually.

dx.doi.org/10.1021/jp2008682 |J. Phys. Chem. B 2011, 115, 8832–8844

As is mentioned above, hyperbranched polymer is a globule-like polymer which creates more chances for the groups of polymer to interact with the environment than linear polymer. The CH_3 groups are of the highest freedom among all the groups in the polymer. Upon heating, the system begins to exclude water from polymer. If there are still some water molecules, CH_3 groups can always interact well with them. So no intermediates can be observed in the variation of CH_3 groups during heating. But carbonyl groups lie in a relatively restricted position and experience gradual changes. During the cooling process, water molecules came back to surround the polymer. Still due to the freedom of the CH_3 groups, they can interact with water first. With the diffusion of water into the polymer, the CH_3 groups hydrate with water gradually. The C═O···D—N hydrogen bonds are relatively hard to be broken only with enough water. It is an assumption that the hydration of CH_3 groups and H-bonds of tertiary amide groups with only water are preparing for the breakage of C═O···D—N hydrogen bonds. However, it should be further proved and elaboration of this point will be presented later in the text.

Table 1. LCSTs Ranges Arising from Different Vibration Bands Determined by PCMW

	LCST/°C	
freq/cm^{-1}	heating	cooling
2985	32.5	31
2962	32	32
2944	32	29.5
2925	32.5	32
2883	32	30.5
2865	32	32

3.3. Perturbation Correlation Moving Window (PCMW) Analysis. PCMW is a newly developed technique whose basic

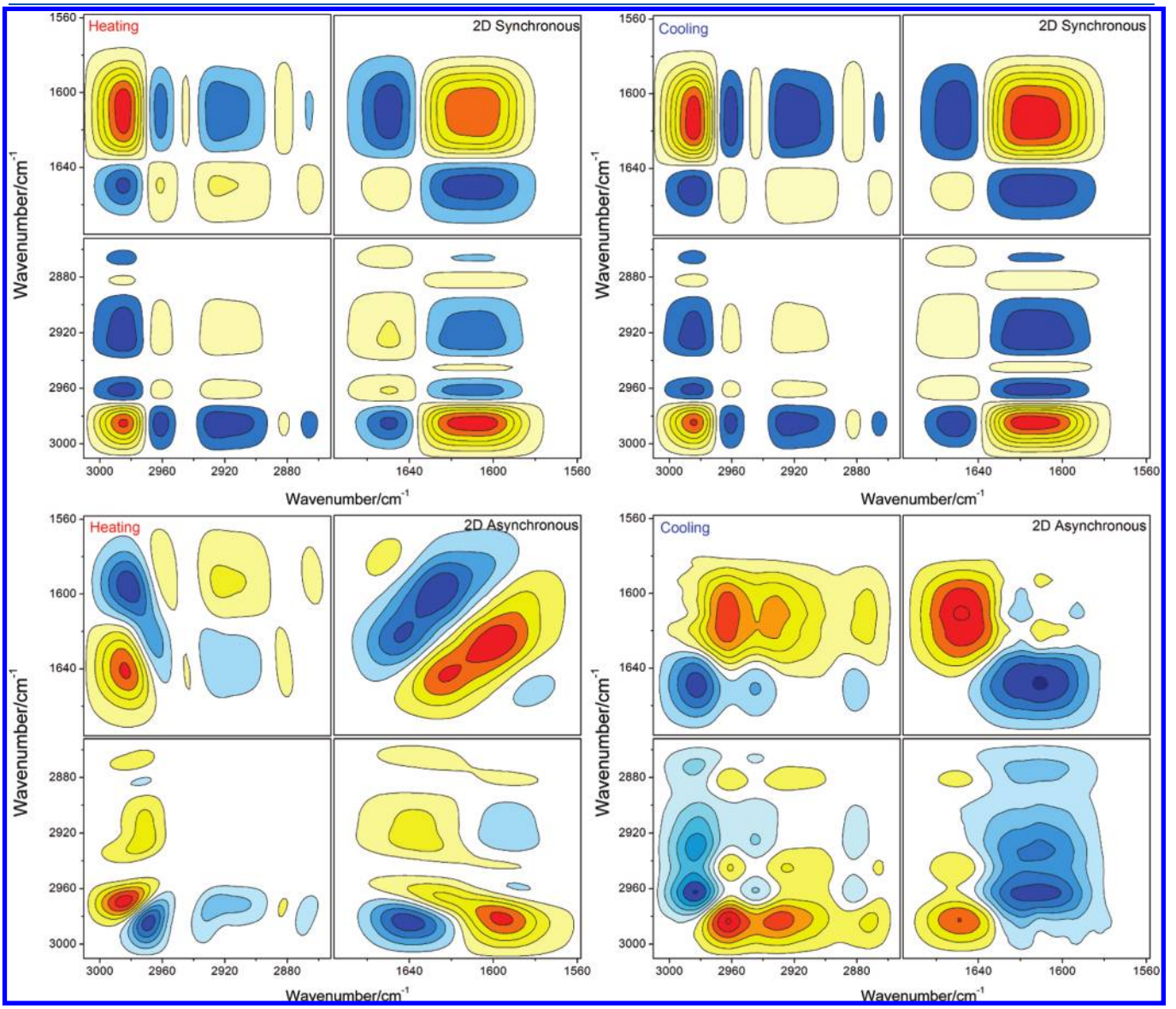

Figure 10. 2D synchronous and asynchronous spectra of 10 wt % HPEI-IBAm in D_2O from all spectra between 29.5 and 34.5 °C during heating (top) and cooling (bottom). Herein, warm colors (red and yellow) are defined as positive intensities, while cool colors (blue) as negative ones.

dx.doi.org/10.1021/jp2008682 |J. Phys. Chem. B 2011, 115, 8832–8844

Table 2. Tentative Band Assignments of HPEI-IBAm According to 2Dcos during Heating and Cooling Respectively

heating				cooling			
freq/cm^{-1}	assignment	freq/cm^{-1}	assignment	freq/cm^{-1}	assignment	freq/cm^{-1}	assignment
2985	ν_{as}(hydrated CH_3)	2867	ν_s(dehydrating CH_3)	2985	ν_{as}(hydrated CH_3)	1650	ν(C═O···D−N)
2967	ν_{as}(dehydrated CH_3)	1650	ν(C═O···D−N)	2962	ν_{as}(dehydrated CH_3)	1625	ν(C═O···D_2O)
2944	ν_{as}(hydrated CH_2)	1643	ν(D-O−D···C═O···D−N)	2944	ν_{as}(hydrated CH_2)	1619/1610	ν(C═O···D_2O)
2935	ν_{as}(dehydrating CH_2)	1625	ν(C═O···D_2O)	2925	ν_{as}(dehydrated CH_2)	1600	ν(C═O···2D_2O)
2925	ν_{as}(dehydrated CH_2)	1600	ν(C═O···2D_2O)	2883	ν_s(dehydrated CH_3)		
2883	ν_s(dehydrated CH_3)			2867	ν_s(dehydrating CH_3)		

principles can date back to conventional moving window proposed by Thomas,[55] and later Morita[56] improved this technique to much wider applicability through introducing the perturbation variable into correlation equation in 2006. Besides its original ability in determining transition points as conventional moving window did, PCMW can additionally monitor complicated spectral variations along the perturbation direction.

Figure 9 shows PCMW synchronous and asynchronous spectra generated from all the spectra during heating and cooling between 27 and 39 °C with an interval of 0.5 °C. For determination of transition point during the heating and cooling process, PCMW synchronous spectra is carefully studied and detailed information is provided in Table 1. Temperature transition points of three CH stretching bands at 2985, 2944, and 2833 cm^{-1} show a small hysteresis, which is consistent with the conclusion obtained above.

Furthermore, PCMW spectra can monitor complicated spectral variations along the temperature direction combining the signs of synchronous and asynchronous spectra by the following rules: positive synchronous correlation represents spectral intensity increasing, while a negative one represents decreasing; positive asynchronous correlation can be observed for a convex spectral intensity variation while negative one can be observed for a concave variation.[56] According to these rules, we can conclude from the PCMW spectra that, during the heating process, the CH regions of 3010−2968, 2949−2934, and 2890−2872 cm^{-1} as well as the C═O region of 1640−1580 cm^{-1} exhibit anti-S-shaped intensity changes, accompanied by the regions of 2968−2949, 2934−2890, 2872−2854, and 1675−1640 cm^{-1} exhibit an S-shaped transition. The cooling process is just the opposite.

In addition, from the asynchronous spectra, it can be observed that all the groups respond to temperature in the range of 30−34 °C during heating and 29.5−34 °C during cooling, which will provide information for 2D correlation analysis.

3.4. Two-Dimensional Correlation Analysis. 2Dcos is a mathematical method whose basic principles were first proposed by Noda in 1986.[57] Up to the present, 2Dcos has been widely used to study spectral variations of different chemical species under various external perturbations (e.g., temperature, pressure, concentration, time, electromagnetic).[58] Due to the different response of different species to external variable, additional useful information about molecular motions or conformational changes can be extracted which cannot be obtained readily from conventional 1D spectrum.

Based on the analysis of PCMW, all the FT-IR spectra between 29.5 and 34.5 °C with an increment of 0.5 °C are applied to generate the 2Dcos spectra. Figure 10 presents the 2Dcos synchronous and asynchronous spectra of HPEI-IBAm during heating and cooling process. 2D synchronous spectra provide information about simultaneous changes between two wavenumbers. Derived from Figure 10, bands at 2985, 2883, 1625, and 1600 cm^{-1} all show positive cross peaks, indicating their similar sensitivities to perturbation. Combined with original spectra, we found out that the intensities of these bands all decrease during heating while increase in the cooling process. While cross peaks between those bands at 2985 and 2960/2925 cm^{-1} show a negative pattern, implying opposite changes of 2960/2925 to 2985 cm^{-1}. Similarly, we can deduce that intensity of 2960 and 2925 cm^{-1} increased upon heating and decreased upon cooling. 2D asynchronous spectra can enhance resolution of the spectra. Several bands such as 1643 cm^{-1} and 1619/1610 cm^{-1} that cannot be determined by 1D FT-IR are obtained. For clarity, all bands detected from 2Dcos spectra during heating and cooling process and their tentative assignments are listed in Table 2.

For expository convenience, the sequence order of HPEI-IBAm during heating−cooling process will be illustrated in the ν(C═O) and ν(CH) regions separately. The judging rule of the sequence can be summarized as Noda's rule—that is, if the cross peaks (ν_1, ν_2, and assume $\nu_1 > \nu_2$) in synchronous and asynchronous spectra have the same sign, the change at ν_1 may occur prior to ν_2, and vice versa. Based on the judging rule, the sequence order of each region is described below.

1. C═O Region. Heating: 1643 > 1650> 1600 > 1625 cm^{-1}; cooling: 1610 > 1619 > 1650 cm^{-1} (where ">" means prior to or earlier than).

The carbonyl groups can form hydrogen bonds with water molecules or D—N of amide groups in aqueous solution. As mentioned above, 1650, 1625, and 1600 cm^{-1} are assigned to hydrogen bonds of C═O···D—N, and singly and doubly H-bonding of C═O···D_2O, respectively. Considering the discussion of the isosbestic point, during the heating process, hydrogen bonds of C═O···D—N form upon gradual disassociation of C═O···D_2O hydrogen bonds, with intermediates existing. The band at 1643 cm^{-1} is attempted to be assigned as an intermediate component, which may be attributed to hydrogen bonds of C═O with both D_2O and D—N of amide groups. 1619 and 1610 cm^{-1} are attributed to intermediates of hydrogen bonds between carbonyl groups and water molecules during the phase transition.

According to the sequence in combination with their assignments, changes during phase transition can be described as follows.

During the heating process, the intermediate component first responds upon heating, converting to hydrogen bonds of C═O···D—N, and leads to an increment of 1650 cm^{-1}; and the formation of C═O···D—N hydrogen bonds helps to remove water from hyperbranched polymer, which further

dx.doi.org/10.1021/jp2008682 |J. Phys. Chem. B 2011, 115, 8832–8844

promotes disassociation of strong hydrogen bonds of C═O···D_2O into a weak one.

Upon cooling, H-bonds between C═O and water molecules are strengthened with water diffusion into polymer. Interestingly, the strong hydrogen bonds make a response followed by the weaker one, which seems abnormal. Taking the specific structure of hyperbranched polymer into account, as terminal groups, amide I are located on periphery of the globule-like polymer. When the temperature reaches LCST, inter/intra-hydrogen bonds of amide I start to form. If macromolecules form aggregates with each other after phase transition, the amide I groups on the periphery of the aggregates will be attacked more easily, particularly those that do not participate in the H-bonding of C═O···D—N. These amide I groups remain H-bonding with water molecules more or less. The higher degree of H-bonding with water can somewhat indicate a higher degree of freedom. Then one can imagine that, when cooling down, water returns to surround the aggregates, and strong hydrogen bonds of C═O with water will be strengthen first followed by the weaker one. Then the C═O···D—N hydrogen bonds begin to disassociate.

2. C−H Region. Heating: 2967 > 2935> 2883 > 2925 > 2985 cm^{-1}; cooling: 2944 > 2883> 2985 > 2925 > 2962 cm^{-1} (where ">" means prior to or earlier than).

Combined with the assignments from Table 2, the sequence can be described as follows:

Heating: ν_{as}(dehydrated CH_3) > ν_{as}(dehydrating CH_2) > ν_s(dehydrating CH_3) > ν_s(dehydrated CH_3) > ν_{as}(dehydrated CH_2) > ν_{as}(hydrated CH_3).

Cooling: ν_{as}(hydrated CH_2) > ν_s(dehydrated CH_3) > ν_{as}-(hydrated CH_3) > ν_{as}(dehydrated CH_2)> ν_{as}(dehydrated CH_3).

The C−H groups are defined as the hydrophobic moiety of the polymer. During the phase transition process, the C−H groups will experience states of hydration or dehydration. Upon heating, dehydration of C−H groups results in red shift. During the cooling process, the frequency of C−H groups undergoes blue shift with hydration with water.

Carefully considering the sequence from the 2Dcos analysis, one can discern that the less hydrated $\nu_{as}(CH_3)$ dehydrated followed by dehydrating $\nu_{as}(CH_2)$ and $\nu_s(CH_3)$ during the heating process. The band at 2967 cm^{-1} has a higher degree of hydration than that at 2962 cm^{-1}, an assignment to more dehydrated $\nu_{as}(CH_3)$. From the isosbestic point determination, we claim that there is an isosbestic point at 2970 cm^{-1} of enlarged C−H region during heating. So, no intermediates should exist in this region during heating. The phenomena of an emergence of 2967 cm^{-1} will be discussed later in the text.

Referring to the cooling process, the CH_2 groups respond to temperature perturbation earlier than CH_3 groups. Hyperbranched polymer is an imperfect branched polymer with defects involving its structure compared to the dendrimer. Upon cooling, diffusion of water into the polymer may first attack these defects and then result in a first response of CH_2 groups.

3. C═O and C−H Region. Heating: 1648 > 1600 > 2967 > 2935 > 2867 > 2883 > 2925 > 2985 > 1625 cm^{-1}.

Cooling: 2944 > 2883 > 2985 > 1600 > 1625> 1648 > 2925 > 2962 cm^{-1}.

The sequence here can be simplified as

Heating: C═O > C−H; cooling: C−H > C═O

The C═O and C−H region is analyzed to find out the sequence of C═O and C−H during temperature perturbation. As temperature increases, carbonyl groups respond first with the conversion of hydrogen bonds and exclude water from polymer, then C−H groups begin to dehydrate and promote further conversion of H-bonds. Upon cooling, the driven force of the revival is the hydration of CH groups followed by the transformation of hydrogen bonds of carbonyl groups.

In a word, the dissociation of C═O···D_2O during the heating process results in the exclusion of water from the polymer preparing for the dehydration of the C−H groups; during the cooling process, hydration of the C−H groups is a preparation for the breakage of C═O···D—N hydrogen bonds. The so-called preparation work results in the two isosbestic points shown in Figure 8 as discussed above.

Table 3. Hydrodynamic Radius of Hyperbranched Polymer with Different Concentrations during the Heating Process

	$R_{h,app}$/nm			$R_{h,app}$/nm	
temp/°C	1 mg/mL	10 mg/mL	temp/°C	1 mg/mL	10 mg/mL
25	2.859	2.963	33	2.431	1396
26	2.741	2.895	34	2.331	1615
27	2.727	2.867	35	2.283	1715
28	2.603	2.789	36	2.241	
29	2.657	2.647	37	227	
30	2.465	2.631	38	558.7	
31	2.491	2.668	39	702.5	
32	2.409	762.3	40	720.4	

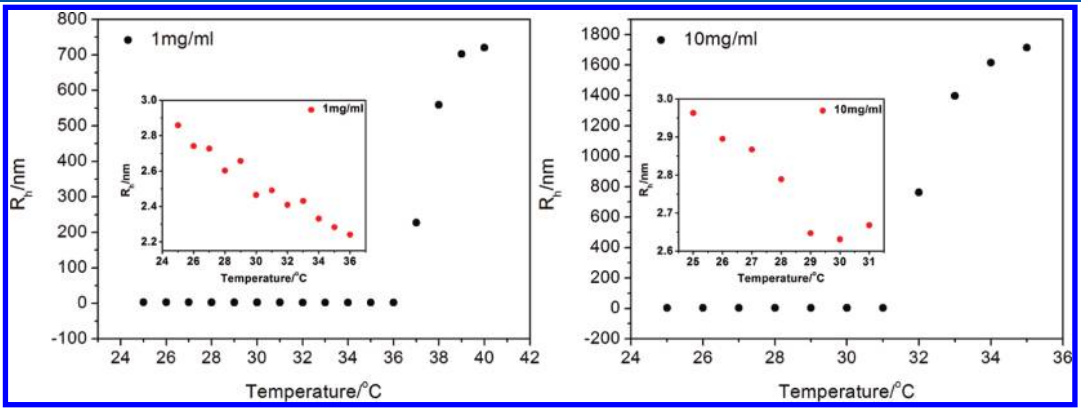

Figure 11. Size changes of HPEI-IBAm particle with different concentrations in H_2O during heating process. The inset shows the temperature dependence of size below LCST.

dx.doi.org/10.1021/jp2008682 |*J. Phys. Chem. B* 2011, 115, 8832–8844

3.5. DLS Measurement. DLS was carried out with the concentration of 1 mg/mL (0.1 wt %) and 10 mg/mL (1 wt %) of HPEI-IBAm aqueous solution from 25 to 40 °C and 25 to 35 °C with an interval of 1 °C, respectively. Suitable concentration is chosen for appropriate scattering intensity without interaction among particles before phase transition.

Hydrodynamic radius $R_{h,app}$ values during the heating process are listed in Table 3 and the relevant temperature-dependent curves are presented in Figure 11. For thermosensitive HPEI-IBAm aqueous solution, the higher the concentration is, the lower the LCST achieved.[31] The LCST measured from DLS is 36 and 32 °C for 1 and10 mg/mL, respectively, which are in accordance with the results from turbidity measurement at the same concentration. Hydrodynamic radius $R_{h,app}$ of the polymer in water remains 2−3 nm below LCST, but increases by 100 times abruptly when the temperature reaches its LCST. As temperature increases, $R_{h,app}$ becomes larger and larger but with a smaller increase rate. With an enlarged region of hydrodynamic radius $R_{h,app}$ below LCST from the inset, a decrement of $R_{h,app}$ upon heating is figured out. It can be concluded that the hyperbranched polymer exists in water as a small particle with $R_{h,app}$ of 2−3 nm below LCST, and then shrinks with conformational adjustment. By the way, there is no dehydration occurring according to the temperature-dependent curves of $\nu_{as}(CH_3)$ in Figure 7, as mentioned above. When the temperature reaches its LCST, the small particles start to interact with each other by hydrophobic interaction and hydrogen bonds of inner/intermolecular amide I groups, resulting in the formation of aggregates.

With the conclusion derived from DLS, we can go back to the discussions of the sequence order of CH groups upon cycling up and down. Upon heating, they undergo conformational adjustment below LCST. Consequently, the restricted CH_3 groups due to compact structure are able to continue to hydrate and results in a higher degree hydration state of CH_3 at 2967 cm^{-1}. Then, when the temperature achieves LCST, dehydration is in process and 2967 cm^{-1} dehydrates first.

Finally, molecular mechanism of the phase transition process during the heating−cooling cycle can be obtained. Illustrations are in Schemes 2 and 3.

From Scheme 2, we can see that the hyperbranched polymer exists as small particles originally and shrinks without obvious dehydration at first upon heating. These small particles start to interact with each other and form aggregates later, resulting in

Scheme 2. Illustration for Phase Transition Mechanism of HPEI-IBAm Aqueous Solution during Heating and Cooling

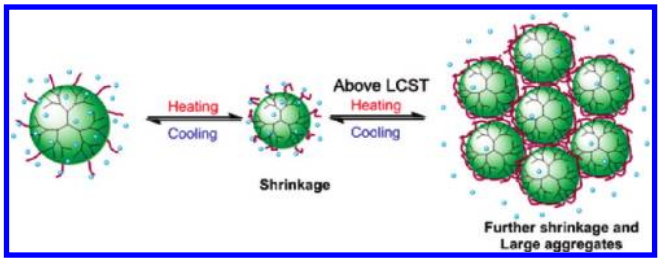

Scheme 3. Supposed Chain Collapse and Revival Thermodynamic Mechanism of HPEI-IBAm Aqueous Solution According to 2D Analysis

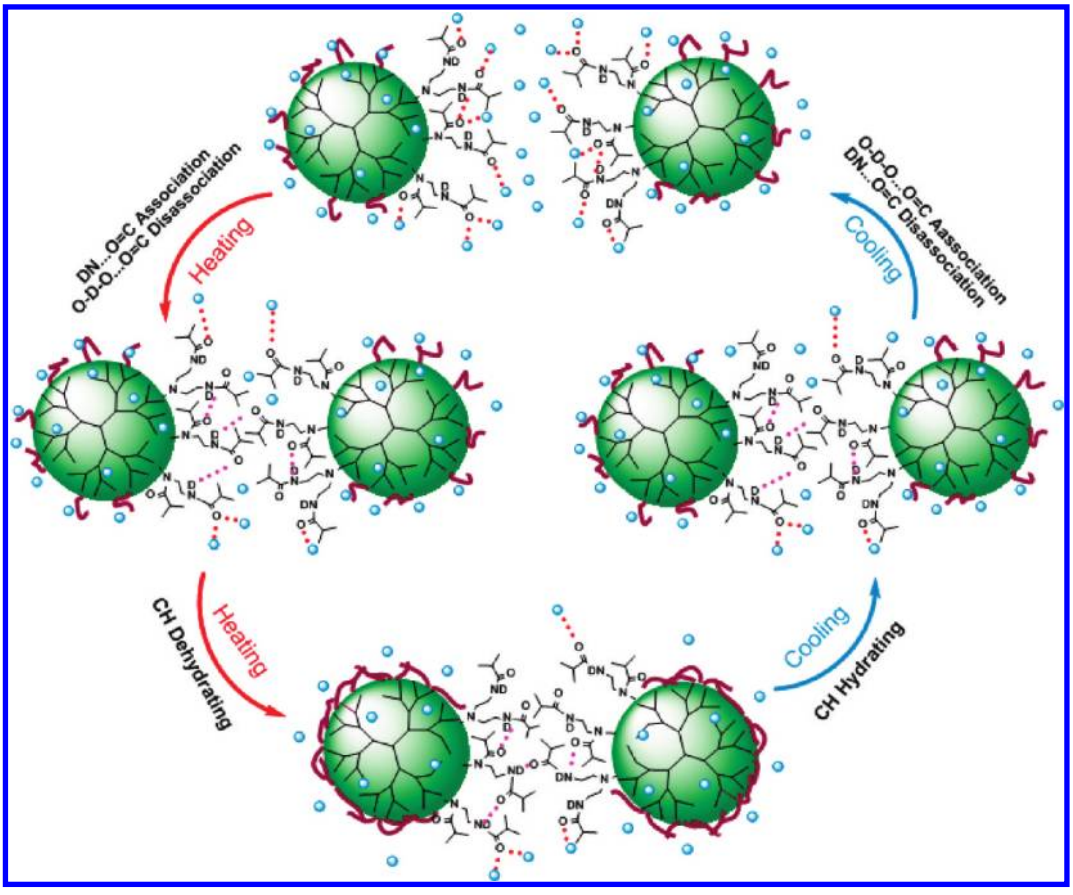

dx.doi.org/10.1021/jp2008682 |J. Phys. Chem. B 2011, 115, 8832–8844

phase transition. For a detailed description of interactions among groups, a diagram is drawn in Scheme 3 wherein only two small particles are shown for representation.

Above LCST of HPEI-IBAm, a heating procedure first leads to the association of C═O···D—N with dissociation of C═O···D_2O preparing for dehydration of C−H groups. While cooling down, the C−H groups interact with water molecules at first and result in a hydration phenomenon, preparing for conversion from C═O···D—N to C═O···D_2O.

It should be pointed out that upon heating the polymer shrinks below LCST first which may lead to a more "dilute solution" relatively compared with its original solution. Then, how can the particles aggregate with each other above LCST?

As is discussed above, with temperature increasing, water molecules will be excluded from the polymer with dehydration of the C−H groups and association of C═O···D—N hydrogen bonds. Thus, the globule-like hyperbranched polymer exhibits as a hydrophobic sphere, which is unstable in water. If the temperature continues to increase, the hydrophobic spheres will gain enough energy to aggregate with each other by hydrophobic interaction to achieve a relatively stable state. Quite different from the hyperbranched polymer, the linear polymer of a long chain, such as linear-PNIPAM with amide groups as its pendent groups, will experience an irregular inner/inter interaction also by dehydration of the C−H groups and association of C═O···D—N hydrogen bonds but this results in a seriously entangled chain system which finally collapses.

4. CONCLUSION

In this paper, we carry out a detailed study on the molecular mechanism of thermal-induced phase transition of HPEI-IBAm. An in situ tracing by FT-IR measurement was performed together with a macroscopic perspective by DLS.

The second-derivative spectra and Gaussian fitting were adopted to separate different components of the overlaid spectra. 1648, 1625, and 1600 cm^{-1} are assigned to H-bonded C═O···D—N, and singly and doubly H-bonded carbonyl groups with water molecules, respectively. The difference of absorption coefficient of the three components results in a decrease of the total area of the amide I region. Due to the high specific area of the hyperbranched polymer, as well as tertiary amide I groups, a better revival of C═O···D—N hydrogen bonds is gained compared to linear-PNIPAM solution. Quantitative analysis of the C−H region provides that CH_3 groups in the outer position of the globule-like polymer have a higher degree of freedom than CH_2 groups.

The isosbestic points that exist at 1638 and 2970 cm^{-1} in the heating and the cooling process, respectively, provide that the CH_3 groups are of the highest freedom to interact with water surrounded upon cycling up and down. The results are consistent with 2D analysis. During the heating process, hydrogen bonds of C═O···D—N form followed by dissociation of C═O···D_2O and exclude water from polymer, preparing for dehydration of CH groups and further promoting the weakening of C═O···D_2O hydrogen bonds. Upon cooling, hydration of CH_2 groups occurs at first as a preparation for the formation of C═O···D_2O H-bonds. After that, H-bonded C═O···D_2O are strengthened upon the breakage of C═O···D—N hydrogen bonds.

In summary, the thermosensitive hyperbranched polymer dissolves in water as small particles of 3 nm at room temperature. Upon heating, the small particles begin to shrink and then aggregate with each other for a relative stable state above LCST. The cooling process is just the opposite. This is the first study of the thermal-induced phase transition mechanism at molecular level with a deep insight into interactions of different groups, especially for a hyperbranched polymer with the basic polymer's extensive applications in biomedical field and its own environmental sensitivity.

AUTHOR INFORMATION

Corresponding Author
*E-mail: peiyiwu@fudan.edu.cn.

ACKNOWLEDGMENT

We gratefully acknowledge the financial support from National Science Foundation of China (NSFC) (20934002, 51073043), the National Basic Research Program of China (No. 2009CB930000).

REFERENCES

(1) Cheng, H.; Yuan, X.; Sun, X.; Li, K.; Zhou, Y.; Yan, D. *Macromolecules* **2010**, *43*, 1143.
(2) Voit, B.; Lederer, A. *Chem. Rev.* **2009**, *109*, 5924.
(3) Gao, C. *Prog. Polym. Sci.* **2004**, *29*, 183.
(4) Inoue, K. *Prog. Polym. Sci.* **2000**, *25*, 453.
(5) Fei, B.; Yang, Z.; Shao, S.; Wan, S.; Xin, J. *Polymer* **2010**, *51*, 1845.
(6) Yates, C. *Eur. Polym. J.* **2004**, *40*, 1257.
(7) Zhou, Y.; Guo, Z.; Zhang, Y.; Huang, W.; Zhou, Y.; Yan, D. *Macromol. Biosci.* **2009**, *9*, 1090.
(8) Sun, X.; Zhou, Y.; Yan, D. *Sci. China, Ser. B* **2009**, *52*, 1703.
(9) Guo, B.; Sun, X. Y.; Zhou, Y. F.; Yan, D. Y. *Sci. China−Chem.* **2010**, *53*, 487.
(10) Zhou, Y.; Yan, D. *Chem. Commun.* **2009**, 1172.
(11) Liu, J.; Huang, W.; Pang, Y.; Zhu, X.; Zhou, Y.; Yan, D. *Langmuir* **2010**, *26*, 10585.
(12) Stiriba, S. E.; Kautz, H.; Frey, H. *J. Am. Chem. Soc.* **2002**, *124*, 9698.
(13) Zhou, Y.; Yan, D.; Dong, W.; Tian, Y. *J. Phys. Chem. B* **2007**, *111*, 1262.
(14) Sun, B.; Lin, Y.; Wu, P.; Siesler, H. *Macromolecules* **2008**, *41*, 1512.
(15) Agut, W.; Brulet, A.; Schatz, C.; Taton, D.; Lecommandoux, S. *Langmuir* **2010**, *26*, 10546.
(16) Plamper, F. A.; Schmalz, A.; Ballauff, M.; Muller, A. H. E. *J. Am. Chem. Soc.* **2007**, *129*, 14538.
(17) Roth, P.; Jochum, F.; Forst, F.; Zentel, R.; Theato, P. *Macromolecules* **2010**, *43*, 4638.
(18) Heskins, M.; J., E.; James, E. *J. Macromol. Sci., Chem.* **1968**, *A2*, 1441.
(19) Maeda, Y.; Nakamura, T.; Ikeda, I. *Macromolecules* **2002**, *35*, 10172.
(20) Yamamoto, K.; Serizawa, T.; Muraoka, Y.; Akashi, M. *Macromolecules* **2001**, *34*, 8014.
(21) Zareie, M. *J. Colloid Interface Sci.* **2002**, *251*, 424.
(22) Liu, H. J.; Zhong, S.; Striba, S. E.; Chen, Y.; Zhang, W. Q.; Wei, L. H. *J. Polym. Sci. Polym. Chem.* **2006**, *44*, 4165.
(23) Luo, S. Z.; Xu, J.; Zhu, Z. Y.; Wu, C.; Liu, S. Y. *J. Phys. Chem. B* **2006**, *110*, 9132.
(24) Haba, Y.; Kojima, C.; Harada, A.; Kono, K. *Macromolecules* **2006**, *39*, 7451.
(25) Haba, Y.; Harada, A.; Takagishi, T.; Kono, K. *J. Am. Chem. Soc.* **2004**, *126*, 12760.
(26) Haba, Y.; Kojima, C.; Harada, A.; Kono, K. *Angew. Chem.* **2007**, *46*, 234.

(27) Kojima, C.; Yoshimura, K.; Harada, A.; Sakanishi, Y.; Kono, K. *Bioconjugate Chem.* **2009**, *20*, 1054.
(28) Kojima, C.; Yoshimura, K.; Harada, A.; Sakanishi, Y.; Kono, K. *J. Polym. Sci. Polym. Chem.* **2010**, *48*, 4047.
(29) Guo, Z.; Zhang, Y.; Huang, W.; Zhou, Y.; Yan, D. *Macromol. Rapid Commun.* **2008**, *29*, 1746.
(30) Sun, X.; Zhou, Y.; Yan, D. *Macromol. Chem. Phys.* **2010**, *211*, 1940.
(31) Liu, H.; Chen, Y.; Shen, Z. *J. Polym. Sci., Part A: Polym. Chem.* **2007**, *45*, 1177.
(32) Liu, X.; Cheng, F.; Liu, H.; Chen, Y. *Soft Matter* **2008**, *4*, 1991.
(33) Liu, X.; Cheng, F.; Liu, Y.; Li, W.; Chen, Y.; Pan, H.; Liu, H. *J. Mater. Chem.* **2010**, *20*, 278.
(34) Liu, X.; Cheng, F.; Liu, Y.; Liu, H.; Chen, Y. *J. Mater. Chem.* **2010**, *20*, 360.
(35) Godbey, W.; Wu, K.; Mikos, A. *J. Controlled Release* **1999**, *60*, 149.
(36) Park, K. *J. Controlled Release* **2009**, *140*, 1.
(37) Krämer, M.; Stumbé, J.; Grimm, G.; Kaufmann, B.; Krüger, U.; Weber, M.; Haag, R. *ChemBioChem* **2004**, *5*, 1081.
(38) Maeda, Y.; Kubota, T.; Yamauchi, H. *Langmuir* **2007**, *23*, 11259.
(39) Maeda, Y.; Mochiduki, H.; Ikeda, I. *Macromol. Rapid Commun.* **2004**, *25*, 1330.
(40) Guo, Y.; Sun, B.; Wu, P. *Langmuir* **2008**, *24*, 5521.
(41) Maeda, Y.; Yamauchi, H.; Kubota, T. *Langmuir* **2009**, *25*, 479.
(42) Gu, W.; Wu, P. *Anal. Sci.* **2007**, *23*, 823.
(43) Yim, H.; Kent, M.; Mendez, S.; Balamurugan, S.; Balamurugan, S.; Lopez, G.; Satija, S. *Macromolecules* **2004**, *37*, 1994.
(44) Okada, Y.; Tanaka, F. *Macromolecules* **2005**, *38*, 4465.
(45) Ahmed, Z.; Gooding, E.; Pimenov, K.; Wang, L.; Asher, S. *J. Phys. Chem. B* **2009**, *113*, 4248.
(46) Lai, H.; Wu, P. *Polymer* **2010**, *51*, 1404.
(47) Zhou, Y.; Huang, W.; Liu, J.; Zhu, X.; Yan, D. *Adv. Mater.* **2010**, *22*, 4567.
(48) Cheng, H.; Wang, S.; Yang, J.; Zhou, Y.; Yan, D. *J. Colloid Interface Sci.* **2009**, *337*, 278.
(49) Cheng, H.; Shen, L.; Wu, C. *Macromolecules* **2006**, *39*, 2325.
(50) González-Benito, J.; Koenig, J. L. *Macromolecules* **2002**, *35*, 7361.
(51) Berquier, J.-M.; Arribert, H. *Langmuir* **1998**, *14*, 3716.
(52) Cheng, H.; Shen, L.; Wu, C. *Macromolecules* **2006**, *39*, 2325.
(53) Skrovanek, D.; Howe, S.; Painter, P.; Coleman, M. *Macromolecules* **1985**, *18*, 1676.
(54) Berlett, B. S.; Levine, R. L.; Stadtman, E. R. *Anal. Biochem.* **2000**, *287*, 329.
(55) Thomas, M.; Richardson, H. *Vib. Spectrosc.* **2000**, *24*, 137.
(56) Morita, S., H.; Noda, I.; Ozaki, Y. *Appl. Spectrosc.* **2006**, *60*, 398.
(57) Noda, I. *Bull. Am. Phys. Soc* **1986**, *31*, 520.
(58) Noda, I. *J. Mol. Struct.* **2008**, *883*−*884*, 2.